Rubber-like tensile behaviour of yielded high-impact polystyrene

L. Castellani and C. Maestrini
Montedipe Research Centre, Via G. Taliercio 14, Mantova, Italy
(Received 7 November 1988; revised 9 January 1990; accepted 12 February 1990)

The tensile stress–strain properties of yielded high-impact polystyrene (HIPS) have been investigated at room temperature. Two HIPS samples were considered, having different rubber-phase particle sizes and morphologies. Specimens have been subjected to two subsequent tensile test runs, the first one to produce the yielded matter and the second one to test it. Different amounts of yielded matter content in the specimens and different strain rates for yielded matter production were examined by varying the test conditions in the first run. Yielded HIPS exhibits a rubber elastic stress–strain behaviour, which has been interpreted by assuming that a rubber-like material, proportional in amount to the plastic deformation, is present in the specimens as a consequence of the yielding process.

(Keywords: high-impact polystyrene; yielding; rubber elasticity; crazing)

INTRODUCTION

In glassy polymers whose dominant plastic deformation mechanism is crazing, a few crazes (frequently a single craze) are typically observed at the crack tip before fracture[1]. Crack propagation occurs within the fibrillar structure of the craze, through the breakdown of craze fibrils. As Kambour pointed out[2], 'fracture in glassy polymers may be termed the making and breaking of craze material'.

During investigations on crazes at the crack tip in poly(methyl methacrylate) (PMMA), which were performed by means of optical interferometry, Kambour[2] observed that a 'crack-tip craze' can be closed and re-opened in a reversible way by varying the applied stress: the craze elastic extensibility was found to be high, equal to about 100%. More recently, similar investigations conducted by Schirrer[3] confirmed an extension ratio of about 2 for a crack-tip craze between the 'closed' state (stress = 0) and the fully extended state (stress close to the critical value for crack propagation).

In the assessment of the various contributions to fracture energy, it is therefore necessary to take into account the elastic strain energy stored in the craze, and subsequently dissipated during fibril breakdown. According to Kambour[2] this contribution can be estimated to be about 40% of the nominal Griffith fracture energy of the material, and appears therefore to be important.

In the fracture of many rubber-toughened polymers, like high-impact polystyrene (HIPS) and acrylonitrile–butadiene–styrene (ABS), crack propagation is also preceded by crazing at the crack tip. Crazes in these materials are of course much smaller than those which can be observed in homopolymers: typically not a single craze is observed at the crack tip, but a more or less diffuse zone of 'stress-whitened' material, in which a large number of small crazes are present.

It has been verified, however, that craze structure is the same in rubber-reinforced polymers and in homopolymers[4]. Moreover, also for rubber-toughened materials, fracture propagation occurs inside the fibrillar craze structure through fibril breakdown, as can be observed for example in scanning electron microscope (SEM) micrographs of fracture surfaces in HIPS[5].

For a deeper understanding of the deformation micromechanisms that take part in the fracture of rubber-toughened polymers, a study of the mechanical behaviour of the yielded material appears therefore to be useful. Such an investigation would provide information on the effects of the yielded matter structure on the toughness of the material; moreover, indications could be obtained about the mechanical behaviour of crazes themselves. During the work described here, the tensile stress–strain behaviour of yielded HIPS has been investigated: HIPS was chosen because crazing is the only yielding mechanism for this material at room temperature.

MATERIALS

Two HIPS samples, A and B, have been considered: their main characteristics are listed in *Table 1*. It can be observed that:

(a) molecular weight (M_w) and molecular-weight distribution (M_w/M_n) of the polystyrene (PS) phase are about the same for the two materials;

(b) total amounts of rubber phase are equivalent—this was obtained by blending with suitable amounts of PS homopolymer in a single screw extruder at 180°C;

(c) polybutadiene (PB) content is different in the two samples—this corresponds to different microstructures of the rubber-phase particles (see *Figure 1*);

(d) dispersed particle sizes are very different—mean particle diameter in sample B is about five times smaller than in A.

Transmission electron microscope (TEM) micrographs of the two samples are reported in *Figure 1*; sample A shows the typical 'salami' structure, sample B has smaller

0032-3861/90/122278-09

Table 1 Characteristics of the investigated HIPS samples

	PS phase		PB total amount (%)	Rubber phase	
Material	$M_w \times 10^{-3}$	M_w/M_n		Total amount (%)	Particle diameter (μm)
Sample A	160	2	7.0	20	1.6
Sample B	170	2	8.5	20	0.3

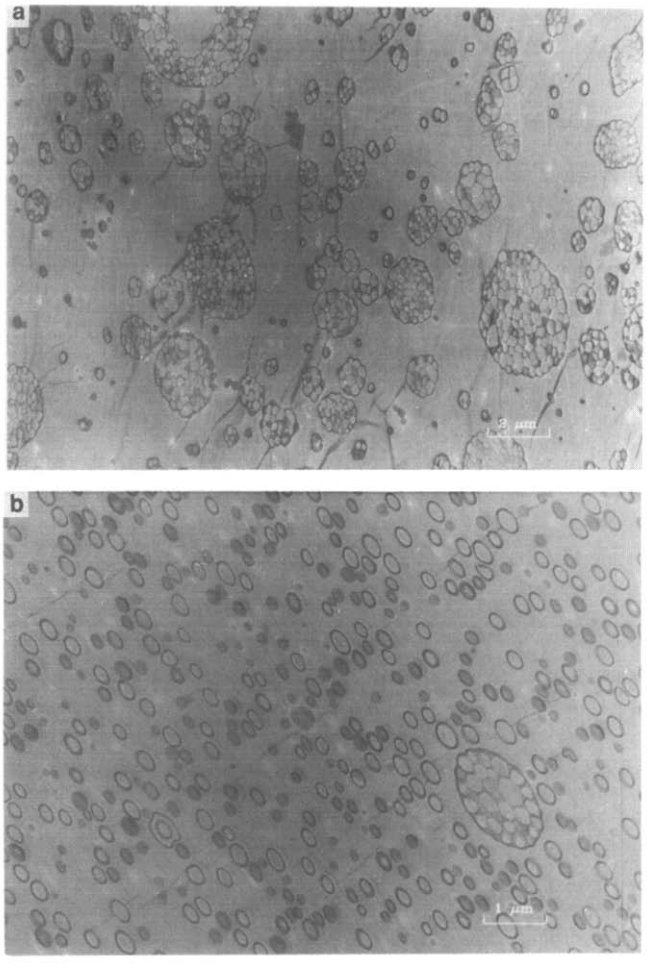

Figure 1 TEM micrographs of the two HIPS samples: (a) sample A; (b) sample B

particles of the so-called 'core–shell' type. Basic differences between sample A and sample B are therefore in dispersed-phase particle size and morphology: PS matrix and rubber-phase amount are nearly equal in the two cases.

EXPERIMENTAL

Experimental investigations were carried out by means of tensile tests performed at room temperature (23°C) on injection-moulded specimens having constant rectangular cross-section ($12.7 \times 3.2\,mm^2$). A servo-hydraulic Zwick-Rel 1852 tester and a conventional Instron tester have been used. The force was measured by piezoelectric or strain-gauge load cells. Elongation has been determined by measuring the distance between the grips: a fixed starting specimen length (i.e. distance between grips) of 78.8 mm has been used. Specimen length will be identified with the distance between testing grips throughout this paper.

Each specimen has been subjected to two subsequent tensile test runs:

(a) run I, in which specimens were strained up to a deformation greater than the yield drop strain but smaller than the breaking strain; and

(b) run II, in which the stress–strain characteristics of yielded material produced in run I have been measured.

Between the two runs each specimen has been removed from the testing grips and allowed to stay at zero stress for a fixed amount of time.

The test variables that have been considered are:

(i) maximum specimen length in run I, $L_{max,I}$—as mentioned above $L_{max,I}$ ranged from values slightly higher than the one corresponding to yield drop to values close to rupture;

(ii) strain rate in run I, $\dot{\varepsilon}_I$ ($\dot{\varepsilon}_I = d\varepsilon_I/dt$, where ε_I is the strain, i.e. the length increment divided by initial length, in run I);

(iii) time between the two runs (during which specimens were disconnected from the tester), Δt;

(iv) specimen length at the starting point in run II, $L_{0,II}$, which was in all cases greater than run I starting length, $L_{0,I}$ ($L_{0,I}$ was equal to 78.8 mm in all cases as said before)—grip positions on the specimens in run I were carefully marked in order to reproduce them exactly in run II (reproducibility within ± 0.2 mm was achieved); and

(v) strain rate in run II, $\dot{\varepsilon}_{II}$.

RESULTS

Figure 2 shows the typical appearance of stress–strain curves obtained in run I and run II. The stress is calculated as the ratio between measured force and specimen cross-sectional area: as is well known[6], the cross-sectional area is a constant during plastic deformation in HIPS. The strain is determined as $\varepsilon = \Delta L/L_0$, where L_0 is equal to $L_{0,I}$ in run I and to $L_{0,II}$ in run II.

Curves obtained in run I are typical HIPS stress–strain curves. The general shape of these curves has been found to be the same for the two samples, whereas the yield

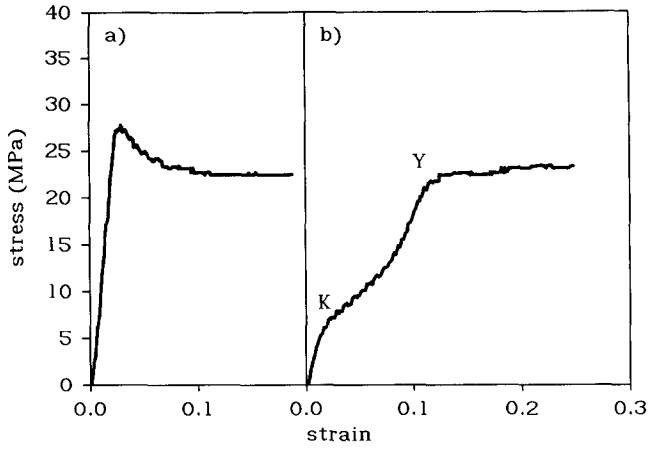

Figure 2 A typical example of stress–strain curves obtained (a) in run I and (b) in run II. Sample A data with $\dot{\varepsilon}_I = 0.12\,s^{-1}$, $L_{max,I} = 93.5$ mm, $\dot{\varepsilon}_{II} = 0.12\,s^{-1}$ (see text). Marks 'Y' and 'K' are referred to in the 'results' subsection on stress–strain characteristics

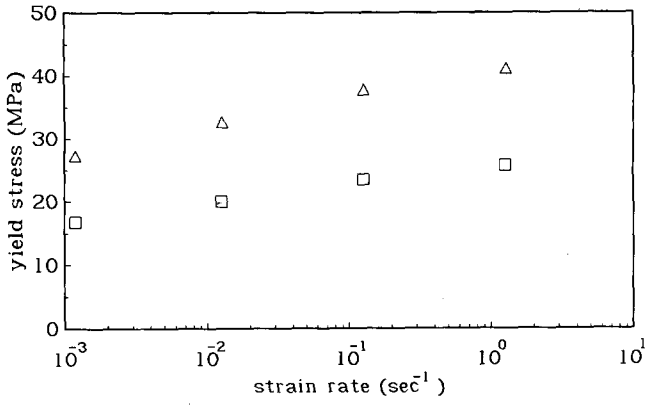

Figure 3 Yield stress vs. strain rate ($\dot{\varepsilon}_I$) for the two samples in run I: (□) sample A; (△) sample B

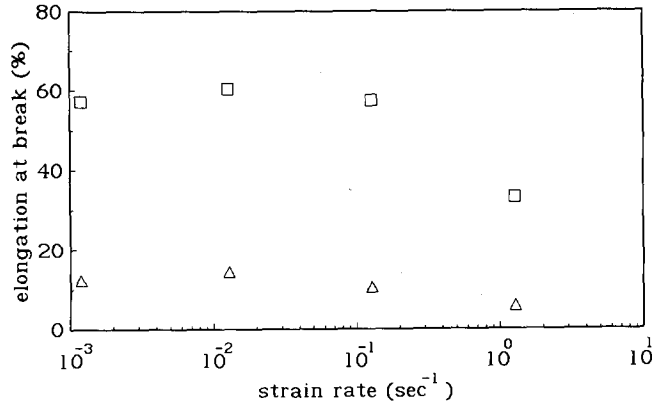

Figure 4 Elongation at break vs. strain rate ($\dot{\varepsilon}_I$) for the two samples in run I: (□) sample A; (△) sample B

stress σ_y and the elongation at break ε_b were different: *Figures 3* and *4* show the average σ_y and ε_b values plotted vs. strain rate ($\dot{\varepsilon}_I$) for the two materials.

Results obtained in run II are described in the following subsections.

Specimen length at the beginning of run II

The length of the yielded specimen before run II ($L_{0,II}$) was found to be variable and, in all cases, greater than the original specimen length before run I ($L_{0,I}$). The experimental variables that can affect $L_{0,II}$ are: rubber-phase structure (sample A or sample B); amount of plastic deformation imposed onto the specimen during run I (that is, $L_{max,I}$); strain rate in run I ($\dot{\varepsilon}_I$); and time elapsed between the end of run I (followed by immediate stress removal from the specimen) and the beginning of run II (Δt).

The effects of Δt on $L_{0,II}$ are described in *Figure 5*, which shows a length vs. time plot (recovery) for a sample A specimen subjected to a generic run I test. The variations in run I parameters ($L_{max,I}$ and $\dot{\varepsilon}_I$) or in the rubber-phase structure (sample A or B) do not affect the qualitative features of this curve. As can be seen in *Figure 5*, a considerable part of the strain is recovered in a few seconds after stress removal: in this time range elastic forces are likely to be responsible for most of the observed recovery. Nevertheless, the recovery process does not seem to reach an end even after times of the order of some days. The same strain–time relationship, characterized by a large initial recovery followed by a slow time-dependent response, was observed by Bucknall during creep and recovery experiments on HIPS[6]. This behaviour can be explained by considering the non-stability of craze structure, which undergoes the phenomenon of craze healing[7]. Craze healing, which causes progressive closure of crazes, has been explained on the basis of fibril coalescence, this being possible because of a particularly high mobility of polymer molecules within the fibrillar structure[8]. In order to measure the stress–strain properties of yielded HIPS, craze healing, which produces structural modifications, has to be avoided, and therefore Δt values must be low. On the other hand, at very low Δt values specimen length is strongly time-dependent (see *Figure 5*) and this would give rise to difficulties in obtaining reproducible experimental conditions. As craze healing in PS at room temperature is known to be a slow process[7–9], we chose a Δt value of 20 min, which was used, unless otherwise specified, in all the experimental tests described in the present work.

As far as the effects of $L_{max,I}$, $\dot{\varepsilon}_I$ and rubber-phase structure on $L_{0,II}$ are concerned, experimental results are illustrated in *Figure 6*. Here $L_{0,II}$ is plotted as a function of $L_{max,I}$ for both the samples, each of them at two different values of $\dot{\varepsilon}_I$. A well defined linear relationship is found between $L_{0,II}$ and $L_{max,I}$: a least-squares regression line is also drawn in *Figure 6*. By extrapolating the regression line, it can be observed that point $L_{0,II} = L_{0,I} =$

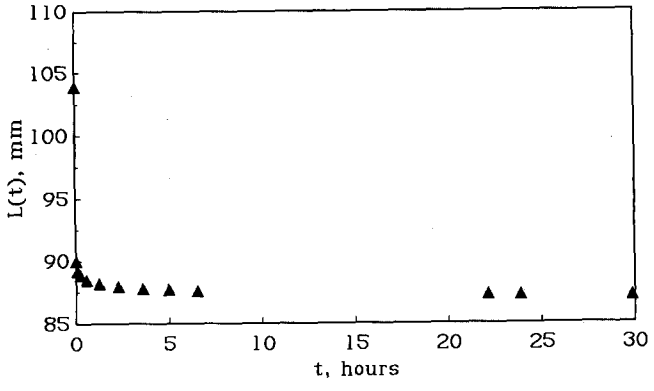

Figure 5 Length as a function of time for a sample A specimen subjected to run I test ($\dot{\varepsilon}_I = 0.01\,s^{-1}$, $L_{max,I} = 103.9$ mm) and disconnected from testing grips at $t = 0$

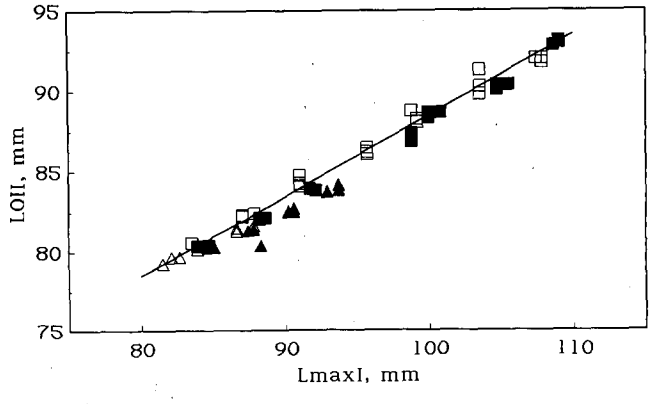

Figure 6 Specimen length at the beginning of run II ($L_{0,II}$) vs. maximum length in run I ($L_{max,I}$): (□) sample A, $\dot{\varepsilon}_I = 1.27\,s^{-1}$; (■) sample A, $\dot{\varepsilon}_I = 0.01\,s^{-1}$; (△) sample B, $\dot{\varepsilon}_I = 1.27\,s^{-1}$; (▲) sample B, $\dot{\varepsilon}_I = 0.01\,s^{-1}$. The full line is the least-squares regression equation: $y = 38.5 + 0.5x$

78.8 corresponds to $L_{max,I}=80.6$. This discrepancy is due to the fact that $L_{max,I}$ is the length of the stressed specimen, while $L_{0,II}$ is the length of the same specimen after stress removal. Therefore, even in the absence of plastic deformation (i.e. in the absence of crazes), a difference between the two quantities has to be expected. The value of 80.6 for $L_{max,I}$, in fact, corresponds to a strain of about 2.3%, which is very close to the yield strain (maximum elastic strain) of HIPS (see *Figure 2*). Within the scattering of experimental data, the relationship between $L_{0,II}$ and $L_{max,I}$ appears not to be influenced by $\dot{\varepsilon}_I$ or by the chosen sample (rubber-phase structure).

Stress–strain characteristics of yielded matter

The main features of the stress–strain curves obtained in run II tests are as follows:

(a) A characteristic point can be observed in each run II curve (it has been marked with 'Y' in *Figure 2b*), which separates two zones exhibiting different mechanical behaviour.

(b) Before point Y a non-linear stress–strain curve is observed, with a strain softening region (marked with 'K' in *Figure 2b*) followed by strain hardening.

(c) After point Y stress is about constant, its value being very close to the one measured at the stop point in run I (stress corresponding to $L_{max,I}$).

Figure 7 shows an example of direct comparison between stress at point Y and stress corresponding to $L_{max,I}$ (sample A data are reported: behaviour of sample B is quite similar). The comparison is made at three different strain rate values ($\dot{\varepsilon}_I$ being equal to $\dot{\varepsilon}_{II}$ in these tests), in order to span an appreciable range of stress values: variations in $L_{max,I}$ alone are in fact producing very little variations in stress level, due to stress being almost constant in run I from yield drop up to the breaking point.

A comparison between specimen length at point Y, hereafter indicated with L_Y, and specimen length at the stop point in run I ($L_{max,I}$) is illustrated in *Figure 8*. Data from sample A and sample B are shown, each of them at two different $\dot{\varepsilon}_I$ values but with the same, constant value of $\dot{\varepsilon}_{II}$.

An equivalence of point Y and point $L_{max,I}$ in terms of both stress and strain results from data reported in *Figures 7* and *8*. Such an equivalence appears not to be affected, within the experimental errors, by rubber-phase morphology or by strain rate.

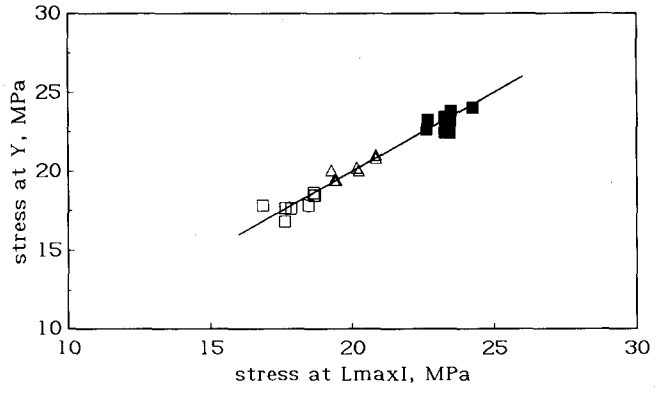

Figure 7 Comparison between stress at point Y (run II) and stress at $L_{max,I}$ (run I). Sample A data are shown with $\dot{\varepsilon}_I=\dot{\varepsilon}_{II}=0.01\,s^{-1}$ (□), $0.12\,s^{-1}$ (△), $1.27\,s^{-1}$ (■). Full line: $y=x$

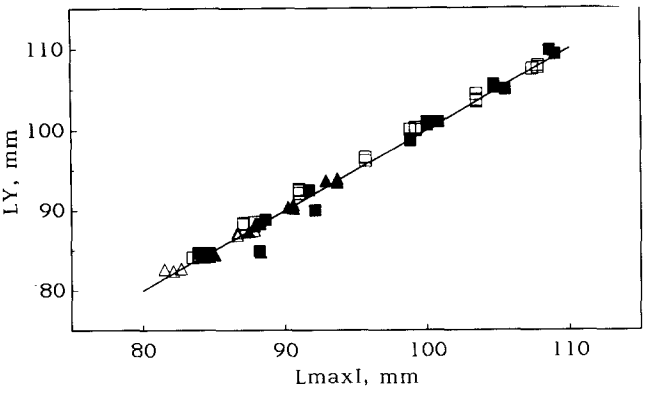

Figure 8 Comparison between specimen length at Y, L_Y (run II), and maximum length reached by same specimen in run I ($L_{max,I}$). Symbols as in *Figure 6*. For all the specimens $\dot{\varepsilon}_{II}=0.12\,s^{-1}$. Full line: $y=x$

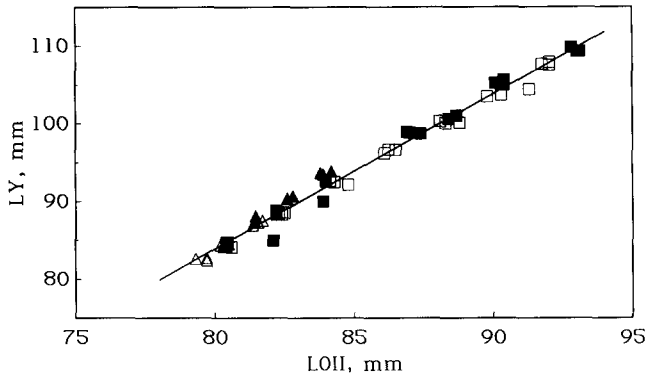

Figure 9 Specimen length at Y, L_Y (run II), plotted vs. starting specimen length in run II ($L_{0,II}$). Symbols as in *Figure 6*. For all the specimens $\dot{\varepsilon}_{II}=0.12\,s^{-1}$. Full line is the least-squares regression equation: $y=-75.2+1.99x$

By considering the results described in *Figures 6* and *8*, a linear relationship has to be expected between L_Y and $L_{0,II}$: *Figure 9* shows the L_Y vs. $L_{0,II}$ plot for the two samples at two different $\dot{\varepsilon}_I$ each. A least-squares regression line is also reported in *Figure 9*. As in the case of the $L_{0,II}$ vs. $L_{max,I}$ relationship shown in *Figure 6*, in *Figure 9* we also find that an extrapolation of regression line to $L_{0,II}=L_{0,I}=78.8$ mm yields an L_Y value greater than $L_{0,I}$, namely equal to 81.3 mm. Also this fact can be ascribed to the elastic extensibility of unyielded material, the slight difference between the value resulting from *Figure 9* (81.3 − 78.8) and the one from *Figure 6* (80.6 − 78.8) probably being due to experimental errors, particularly in measuring L_Y.

Data reported in *Figures 6, 7, 8* and *9*, as was pointed out above, were obtained by using a fixed Δt value equal to 20 min. The relationships between $L_{0,II}$ and $L_{max,I}$ and between L_Y and $L_{0,II}$ are still linear at higher Δt values: for $\Delta t=24$ h $\partial L_Y/\partial L_{0,II}$ is a constant, equal to about 2.5. The slope is higher owing to the fact that $L_{0,II}$ values decrease with increasing Δt: this can be ascribed to craze healing as discussed above. Therefore, the amount of strain recovery that occurs for a given value of Δt appears not to depend on the amount of plastic deformation reached in run I, that is on $L_{max,I}$. Moreover, time effects appear to be slow ($\partial L_Y/L_{0,II}$ increases from ≈ 2, corresponding to $\Delta t=20$ min, to ≈ 2.5 at $\Delta t=24$ h). On the basis of these observations and of the results reported in *Figure 5* we assume that, by fixing the Δt value at 20 min in all the experiments, time-dependent changes in craze

structure, such as those connected with craze healing, can be neglected.

DISCUSSION

The shape of the stress–strain curve of yielded HIPS, as shown in *Figure 2b*, is qualitatively similar, up to point Y, to some of the tensile stress–strain curves obtained by Bucknall and Stevens[10] during cyclic tension–compression tests on HIPS. The characteristic non-linear shape of the curve was ascribed by those authors[10] to the presence of crazes, on the basis of the results obtained by Kambour[11] when measuring the tensile behaviour of a single craze in polycarbonate. In ref. 11 the first 'strain softening' region (corresponding to point K in *Figure 2b*) was explained as a yielding of the fibrillar craze structure, followed by plastic deformation, with strain hardening, of the craze fibrils themselves.

Experimental results reported in *Figures 7* and *8*, however, appear to indicate that the plastic flow processes that are responsible for the plastic deformation of HIPS are resumed at point Y in the very same conditions, in terms of stress and strain, in which they were interrupted at the stop point in run I.

It is generally accepted (see for example ref. 6) that the plastic deformation in HIPS occurs through the following steps:

(i) craze nucléation at the particle–matrix interfaces;
(ii) craze propagation in the plane normal to the applied stress direction;
(iii) craze stop as a result of termination mechanisms, which are connected with the structural and morphological characteristics of rubber-phase particles; and
(iv) craze thickening occurring through the surface drawing of polymer material from the bulk into the craze fibrils[12].

On this basis and considering the equivalence of point Y in run II with the stop point of run I, we formulate the hypothesis that yielded HIPS microstructure, and in particular the number and dimensions of the crazes in the specimen, are the same at the two points. According to this hypothesis, deformation in run II up to point Y does not cause any change in yielded material structure: the stress–strain curve from the beginning of run II up to point Y has therefore to be interpreted as corresponding to the elastic deformation of the yielded material. Consequently, point K cannot be considered as a yield point.

The yielded matter in HIPS includes craze matter plus the rubber-phase particles (or portions of them) which are connecting craze surfaces. As these components are much less stiff than unyielded HIPS, deformation in run II up to point Y, in a first approximation, may be entirely ascribed to yielded matter, the elastic deformation of unyielded phase being neglected. Moreover if we suppose, as seems very reasonable, that the rubber particles that are connecting craze surfaces deform to the same extent as the crazes themselves, we can assume that the extension up to point Y of the yielded matter is equal to the extension of the existing crazes between the initial and the Y points in run II.

As we mentioned in the introduction, the elastic extensibility of a single craze at the crack tip has been investigated for PMMA by Kambour[2] and Schirrer[3] using optical interferometry. The two authors agree in giving a value of about 2 for this maximum elastic extension ratio.

Our experimental results (see *Figures 6* and *9*) allow us to calculate the elastic extensibility of yielded matter, which is equivalent, as we assumed, to the extension ratio of the existing crazes between the point Y and the starting point in run II. It has to be observed that this ratio is not the extension ratio of the material in the fibrils, because in the unloaded buckled state, corresponding to the starting point in run II, there are still voids between the fibrils. However, in order to perform the calculation it is convenient to take into account the volume fraction of uncrazed HIPS that was converted to crazes during run I, which will be indicated with ϕ_c, and the craze fibrils extension ratio λ_c, equal to the inverse of the volume fraction of fibrils in the craze, as defined for example in ref. 12. Using subscripts t, c and m for total specimen, craze and uncrazed material respectively, the following equation for the extension ratio of the total specimen referred to the initial length before run I ($L_{0,I}$) may be written:

$$\lambda_t = \phi_c \lambda_c + (1-\phi_c)\lambda_m \tag{1}$$

According to the approximation of full rigidity of the unyielded material that we made above, we can state that λ_m is equal to 1, and using the subscripts u and s for the unstressed state (corresponding to the starting point in run II) and the fully stressed one (corresponding to point Y), respectively, we can write:

$$\lambda_{tu} = L_{0,II}/L_{0,I} = \phi_c(\lambda_{cu}-1)+1 \tag{2}$$

$$\lambda_{ts} = L_Y/L_{0,I} = \phi_c(\lambda_{cs}-1)+1 \tag{3}$$

From equation (2):

$$\phi_c = (\lambda_{tu}-1)/(\lambda_{cu}-1) \tag{4}$$

and substituting into (3):

$$\lambda_{ts} = \frac{(\lambda_{cs}-1)\lambda_{tu}}{\lambda_{cu}-1} - \frac{1}{\lambda_{cu}-1} + 1 \tag{5}$$

The extension ratio of the existing crazes between the point Y and the starting point of run II, which is the target of this calculation, is clearly given by the ratio $\lambda_{cs}/\lambda_{cu}$. Craze extension ratio between points $L_{0,II}$ and Y is therefore related to total specimen extension ratio between the same points through the following expression:

$$\frac{\partial\lambda_{ts}}{\partial\lambda_{tu}} = \frac{\partial(L_Y/L_{0,I})}{\partial(L_{0,II}/L_{0,I})} = \frac{(\lambda_{cs}-1)}{(\lambda_{cu}-1)} \tag{6}$$

A value for the craze fibrils extension ratio in the fully stressed state λ_{cs} can be obtained from data given by Kramer[12]. According to this author craze fibrils extension ratio at the maximum extension is close to the maximum extensibility of the entanglement network, which he reports to be 4.3 in the case of PS. Setting this value for λ_{cs} and using the experimental value for $\partial L_Y/\partial L_{0,II}$ of about 2, we can evaluate from equation (6) the quantity $\lambda_{cs}/\lambda_{cu}$, which results to be about 1.6.

According to our hypothesis the deformation of crazes in run II up to point Y has to be considered elastic. The high value for the elastic deformability of the existing crazes calculated here is not surprising taking into account the even higher value for the maximum elastic craze extension ratio found by Kambour[2] and Schirrer[3] for PMMA.

The value of 60% obtained for the elastic deformability

of the existing crazes in our case is also an *a posteriori* confirmation that the approximation we made, concerning the rigidity of the unyielded material, is consistent. In fact the value of the maximum elastic deformability of unyielded HIPS is about 2.5% (see *Figures 2, 6* and *9*) and thus can be neglected.

As a consequence of the considerations reported up to now, and because of the strong non-linearity of run II stress–strain curve up to point Y, we attempted to explain the curve itself by means of rubber elasticity theory.

Rubber elasticity equation

The recent formulation of rubber elasticity theory due to Edwards and Vilgis[13] has been chosen. Following ref. 13, the force F per unit volume in uniaxial extension is given by:

$$F/kT = f_s + f_c \tag{7}$$

where k is the Boltzmann constant, T is the absolute temperature, and f_s and f_c are the contributions respectively of entanglements (which are described by means of the 'slip-links' model) and of crosslinks. The contributions f_s and f_c are expressed by the following equations:

$$f_s = N_s\left[\frac{(1+\eta)(1-\alpha^2)\alpha^2 D}{(1-\alpha^2\Phi)^2}\left(\frac{\lambda^2}{1+\eta\lambda^2}+\frac{2}{\lambda+\eta}\right)+\frac{1}{1-\alpha^2\Phi}\left(\frac{\lambda}{(1+\eta\lambda^2)^2}-\frac{1}{(\lambda+\eta)^2}\right)+\eta\frac{D\lambda}{(1+\eta\lambda^2)(\lambda+\eta)}-D\alpha^2\frac{1}{1-\alpha^2\Phi}\right] \tag{8}$$

and

$$f_c = N_c D\left(\frac{1-\alpha^2}{(1-\alpha^2\Phi)^2}-\frac{\alpha^2}{1-\alpha^2\Phi}\right) \tag{9}$$

The functions Φ and D are given by:

$$\Phi = \lambda^2 + 2/\lambda \tag{10}$$

$$D = \mathrm{d}\Phi/\mathrm{d}\lambda \tag{11}$$

and λ is the extension ratio of the considered material ($\lambda = 1+\varepsilon$ where ε is the strain as defined in the preceding section). The other parameters in equations (8) and (9) have the following meanings: N_s is the number of 'slip-links' (entanglements) per unit volume, N_c is the number of crosslinks per unit volume, η is a coefficient giving a measure for the slippage in the slip-links model, and α is a measure of network inextensibility.

In order to attempt a fitting of equation (1) to experimental stress–strain data, some considerations have to be made, which are described in the following sections.

Presence of unyielded HIPS

In the yielded HIPS specimens both a yielded phase (crazes plus rubber particles intersected by one or more craze planes) and an unyielded phase (bulk HIPS) are present. As underlined above, we assume that deformation in run II up to point Y is entirely due to yielded matter, the elastic deformation of unyielded HIPS being neglected. Because of the presence of a rigid phase, the total deformation of the yielded specimen will be lower than the actual deformation of the yielded matter contained in it.

Owing to the characteristic shape of crazes, whose dimensions are much greater in the plane normal to the applied stress direction than in the direction of the applied stress, yielded HIPS may be approximately modelled as a series of layers, alternately highly deformable and completely rigid, lying normal to the applied stress direction. The problem of the deformation of such a series model has been dealt with by Bard *et al.*[14] in the course of a study concerning mechanical properties of styrene–butadiene–styrene (SBS) block copolymers. The relationship between total specimen extension ratio λ_{tot} and the corresponding extension ratio of the deformable phase λ_x has been shown to be given by:

$$\lambda_{tot} = 1 + \phi(\lambda_x - 1) \tag{12}$$

where ϕ is the volume fraction of the deformable phase.

The extension ratio to be introduced in the rubber elasticity equation (equation (1)) is therefore λ_x as obtained from equation (12) and ϕ is a parameter to be determined, together with N_s, N_c, η and α, by fitting equation (1) to the experimental data.

Equation (12) has the same form as equation (1), but the meaning of the parameters involved is different. Here ϕ is the volume fraction of the material that is responsible for the rubber-like behaviour in the unstressed state at the beginning of run II and is not coincident with ϕ_c in equation (1). The extension ratios λ_{tot} and λ_x are also referred to the specimen length at the beginning of run II ($L_{0,II}$), and not to the original unyielded specimen length before run I ($L_{0,I}$), as the extension ratios in the equations (1)–(6) are.

Equilibrium stress

Rubber elasticity theory predicts the equilibrium stress–strain behaviour, that is the stress that exists at a particular strain after any time-dependent contribution has disappeared. A correct comparison of the theory with experimental data would therefore require the measurement of stress–time relationship as a function of strain level, and the consequent determination of the equilibrium stress values. The stress–time relationship in the case of our yielded specimens is exemplified in *Figure 10*, where the stress relaxation curve for a yielded sample A specimen is shown.

Such a behaviour, in which stress is continuously decreasing without reaching a stable level even after

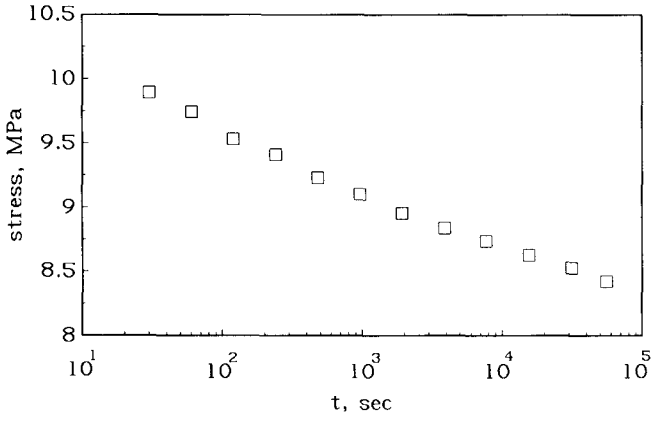

Figure 10 Stress relaxation for a sample A specimen subjected to run I ($\dot{\varepsilon}_I = 0.01\,s^{-1}$, $L_{max,I} = 89$ mm) and to run II ($\dot{\varepsilon}_{II} = 0.01\,s^{-1}$) up to a strain of about 0.09 (corresponding to a length of about 86 mm, which is lower than L_Y): after that strain was kept constant

rather long times (10^5 s), is not unexpected, since plastic deformation of the uncrosslinked PS phase in the specimens, especially within the craze structure where molecular mobility can be enhanced[8], is likely to occur.

A similar problem was encountered by Bard *et al.* in the work mentioned above[14]: the lack of an equilibrium stress level in SBS block copolymers was ascribed to deformation of PS domains. To compare experimental results with the theoretical predictions, Bard and co-workers used the stress measured upon initial application of strain, making the assumption that the time required for strain application was sufficient for most of the relaxation to occur in the rubber phase, but not long enough for significant PS deformation to occur.

In analogy with the procedure followed by those authors[14], we decided to compare rubber elasticity theory with experimental data measured at a finite strain rate, thus assuming that relaxation times of the 'rubber-like phase', which originates the observed stress–strain curve, are much shorter than those giving rise to the stress relaxation shown in *Figure 10*, and that curves obtained at finite strain rate are good approximations to the true equilibrium curves of the 'rubber-like phase'. Such an assumption has to be verified by investigating the effects of strain rate in run II ($\dot{\varepsilon}_{II}$) on the obtained stress–strain data. The fact has to be underlined that no hypotheses have been made, up to now, about the physical nature of the 'rubber-like phase'.

Temperature effects

Rubber elasticity theory describes a peculiar dependence of stress on temperature (Gough–Joule effect), which should be tested in order to verify the rubber-like nature of a material. Such an investigation, however, would require the existence of a definite equilibrium state of the strained specimen. The yielded HIPS specimens tested here, as one can observe in *Figures 5* and *10*, show the presence of strongly time-dependent (and presumably temperature-dependent) phenomena, because of which it would be very difficult to measure the stress–temperature relationship. In view of these difficulties, we did not attempt, in the present work, to investigate temperature effects on the stress–strain behaviour of yielded specimens.

Fitting theory to experimental data

Within the limits of the considerations and assumptions described above, numerical fittings of equation (7) to run II stress–strain data (up to point Y) were carried out in order to evaluate the five parameters (the four ones contained in the original Edwards equation plus parameter ϕ introduced above) as functions of the experimental variables. Minimization of the sum of squared differences between calculated points and experimental data was obtained by means of a computer program based on a simplex algorithm. About 50 discrete stress–strain experimental points were considered for each specimen. The quality of fittings was evaluated by calculating the correlation coefficients R^2 through the usual expression:

$$R^2 = 1 - \frac{\sum (\sigma_c - \sigma_{exp})^2}{\sum (\sigma_{exp} - \langle\sigma_{exp}\rangle)^2} \qquad (13)$$

where σ_{exp} and σ_c are the experimental and computed stress values, and $\langle\sigma_{exp}\rangle$ is the mean value of σ_{exp}. An example of fitting is illustrated in *Figure 11*: the correlation coefficient is equal to 0.992 for the curve shown here. The effects of the different test conditions on the results of fitting calculations are described in the following subsections.

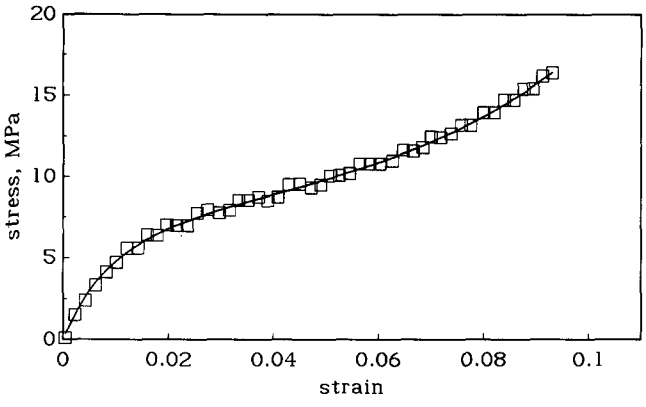

Figure 11 An example of fitting equation (1) (——) to experimental data (sample A) (□). Test parameters: $\dot{\varepsilon}_I = 0.12\,s^{-1}$, $L_{max,I} = 102.4$ mm, $\dot{\varepsilon}_{II} = 0.12\,s^{-1}$. Correlation coefficient $R^2 = 0.992$

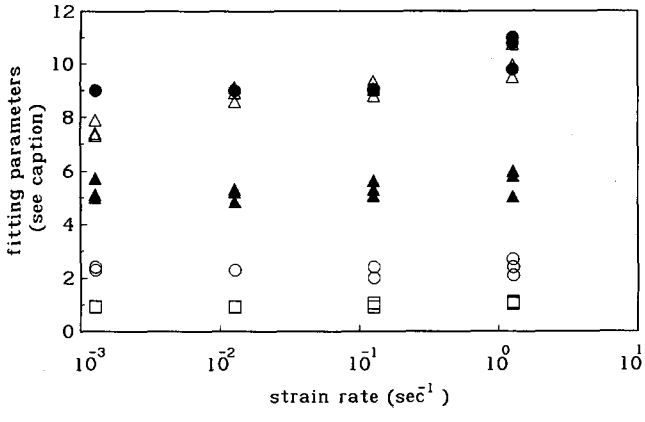

Figure 12 Effects of $\dot{\varepsilon}_{II}$ on parameters resulting from fitting. Sample A data with $\dot{\varepsilon}_I = 0.12\,s^{-1}$, $L_{max,I} = 93.8$ mm. Parameters are plotted against $\dot{\varepsilon}_{II}$ with the following symbols: (△) $N_s kT$ (MPa); (●) $N_c kT$ (MPa) × 10; (▲) $\eta \times 10$; (□) $\alpha \times 10$; (○) $\phi \times 100$. Correlation coefficient $R^2 > 0.99$ in all cases

Effects of $\dot{\varepsilon}_{II}$

In order to evaluate the influence of strain rate in run II on the results of fitting calculations, a number of tests have been conducted on sample A specimens by fixing $L_{max,I}$ (equal to 93.8 mm) and $\dot{\varepsilon}_I$ (equal to $0.12\,s^{-1}$) values, and by varying $\dot{\varepsilon}_{II}$. Results are shown in *Figure 12*, where the parameters resulting from fittings are plotted against $\dot{\varepsilon}_{II}$. In order to show all data in the same graph, ($N_c kT$), α and η values are multiplied by 10 and ϕ values are multiplied by 100 in *Figure 12*. Correlation coefficient (R^2) values greater than 0.99 were obtained for all the experimental curves. All parameters appear to be insensitive to the strain rate in run II, apart from a slight increasing tendency of N_s and N_c: variations of these two parameters are, however, not much greater than the experimental errors. Therefore, the stress–strain curve obtained in run II up to point Y may be considered to be scarcely affected by the strain rate at which run II itself is conducted. This confirms the validity of the previously made assumptions regarding finite strain-rate

measurements. The constant value of ϕ, in particular, encourages us to take this parameter as a measure of the amount of 'rubber-like' material in the specimens.

Following the procedure outlined above, in all the tests described in the following sections we made use of a fixed $\dot{\varepsilon}_{II}$ value equal to $0.12\,s^{-1}$.

Effects of $L_{max,I}$ and $\dot{\varepsilon}_I$

Figure 13 shows the obtained values of parameter ϕ plotted vs. $L_{max,I}$. Data from both samples A and B, each of them at two different strain rates in run I ($\dot{\varepsilon}_I$), are shown. A definite, approximately linear relationship exists between ϕ and $L_{max,I}$: this result is in agreement with the hypothesis that the observed rubber-like behaviour is connected with the elastic deformation of the yielded matter, whose amount is linearly increasing with plastic deformation in run I (i.e. with $L_{max,I}$). Furthermore, one can observe that, within the experimental accuracy, the ϕ vs. $L_{max,I}$ relationship appears not to depend on $\dot{\varepsilon}_I$ or on rubber-phase structure. Results concerning parameters N_s, N_c, η and α are reported in *Figures 14, 15, 16* and *17*. In all cases the values have been found to be insensitive to $L_{max,I}$ and also, within a scattering of about $\pm 10\%$, to $\dot{\varepsilon}_I$ and to the rubber-phase structure variations. Fairly good correlation coefficients were obtained for all the fittings: average, maximum and minimum values corresponding to the two samples at the top $\dot{\varepsilon}_I$ values examined are shown in *Table 2*. Low R^2 values in the case of sample B at high strain rate in run I have been obtained in the low $L_{max,I}$ range: in these conditions the amount of stress whitening, that is the amount of craze matter, is very little, and consequently strain at point Y in run II is low, this giving rise to great scattering in experimental stress–strain measurements.

Results obtained from the application of rubber elasticity theory to our experimental data appear therefore to indicate that a rubber-like material is present in

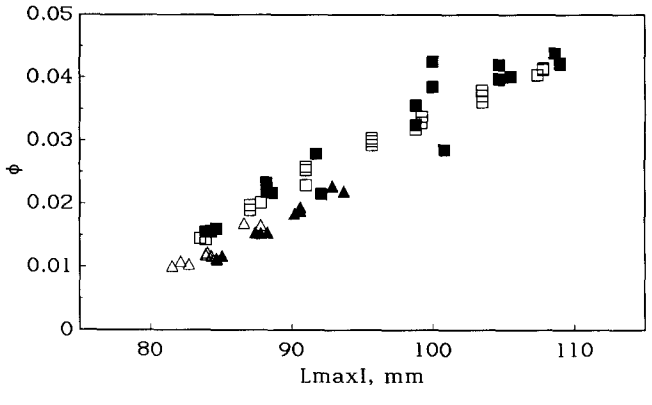

Figure 13 Volume fraction of rubber-like material (ϕ) as a function of $L_{max,I}$. Symbols as in *Figure 6*

Table 2 Values of correlation coefficient R^2 resulting from fitting equation (1) to yielded HIPS stress–strain data

Correlation coefficient R^2	Sample A		Sample B	
	$\dot{\varepsilon}_I = 1.27\,s^{-1}$	$\dot{\varepsilon}_I = 0.01\,s^{-1}$	$\dot{\varepsilon}_I = 1.27\,s^{-1}$	$\dot{\varepsilon}_I = 0.01\,s^{-1}$
Average	0.991	0.988	0.975	0.993
Minimum	0.978	0.980	0.944	0.986
Maximum	0.997	0.997	0.990	0.997

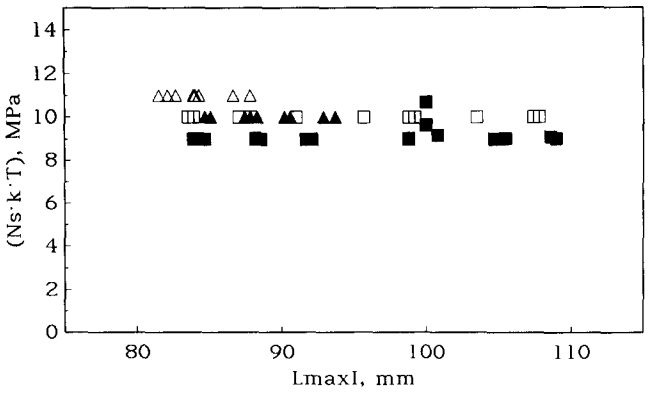

Figure 14 Values for parameter N_s resulting from fitting computations. N_skT is plotted vs. $L_{max,I}$. Symbols as in *Figure 6*

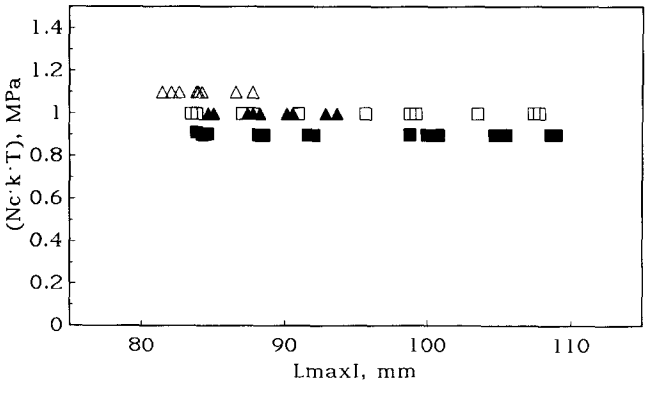

Figure 15 N_c resulting from fitting computations. N_ckT is plotted vs. $L_{max,I}$. Symbols as in *Figure 6*

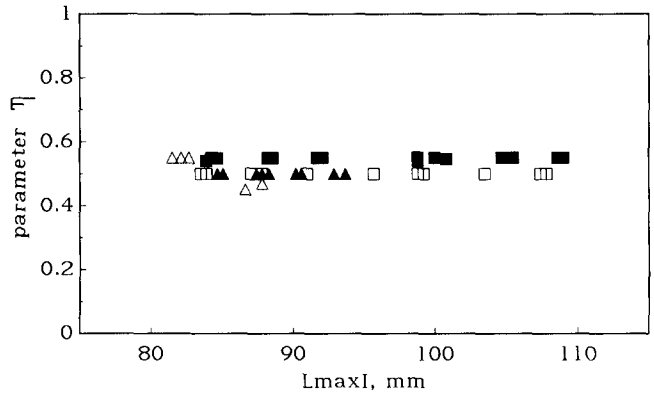

Figure 16 Values for parameter η resulting from fitting, plotted vs. $L_{max,I}$. Symbols as in *Figure 6*

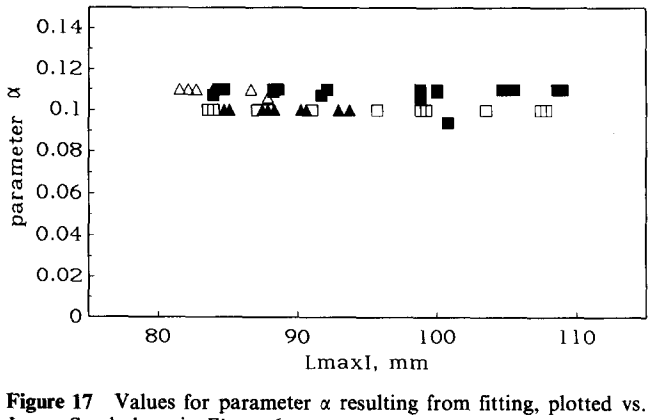

Figure 17 Values for parameter α resulting from fitting, plotted vs. $L_{max,I}$. Symbols as in *Figure 6*

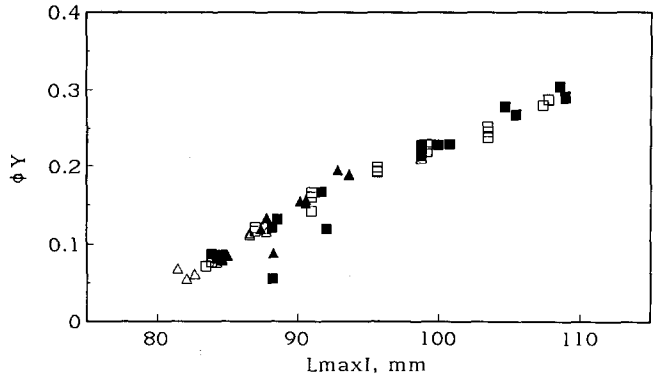

Figure 18 Total yielded matter volume fraction ϕ_Y plotted vs. $L_{max,I}$. Symbols as in *Figure 6*

yielded HIPS as a consequence of yielding and plastic deformation itself.

Structural characteristics of this rubber-like material have been found to be about the same in all the investigated experimental conditions, and therefore appear to be scarcely affected by plastic deformation amount, by strain rate at which plastic deformation occurred and by structure and morphology of rubber-phase particles.

In the preceding discussion the assumption has been made that the rubber-like material is contained in the yielded part of the specimens, unyielded HIPS having been considered as completely rigid. No hypotheses, however, as already pointed out, were made about the nature of the rubber-like material.

In order to obtain indications about this point, it would be useful to know the volume fraction in the specimens of the yielded matter as a whole, i.e. according to our assumptions, the amount of the deformable part of the yielded specimens. The same 'series model' that has been introduced in equation (12) may be used in order to evaluate the total yielded matter volume fraction ϕ_Y in the yielded specimens. This can be done by substituting in equation (12) the experimental $L_Y/L_{0,II}$ values for λ_{tot} and the constant yielded matter extension ratio at Y (equal to about 1.6 as was inferred from equation (6)) for λ_x. The ϕ_Y values obtained in this way are plotted vs. $L_{max,I}$ in *Figure 18*: ϕ_Y vs. $L_{max,I}$ and ϕ vs. $L_{max,I}$ relationships are similar, but ϕ_Y values are about seven times greater than corresponding ϕ values. This is a direct consequence of the fact that the extension ratio at point Y of the crazes, as calculated by equations (1)–(6) and equal to about 1.6, is much lower than the extension ratio at point Y of the material responsible for the rubber-like behaviour, which comes out from the fitting of equation (7) to the experimental data. Hence, rubber-like matter cannot be directly identified with yielded matter.

A problem arises therefore about the origin of the observed stress–strain behaviour. Basically two possible interpretations can be given:

(a) The rubber-like stress–strain curve arises from the elastic deformation of PB rubber contained in the second-phase particles.

(b) The run II curve up to point Y is due to a rubber-like stress–strain behaviour of craze matter.

Hypothesis (a) could provide an explanation for the low ϕ values obtained, because of the composite structure of rubber-phase particles, which can give rise to a 'strain amplification' effect similar to the one described by equation (12). Within this hypothesis it would be necessary to admit that all the applied load, before point Y, is sustained by the rubber phase, and that the amount of load-bearing rubber phase is linearly increasing with craze matter amount. It is difficult, however, to understand how all these features can be insensitive to the large differences in rubber-phase structure and morphology existing between samples A and B, as experimental results appear to indicate.

Hypothesis (b), conversely, would better account for the apparent insensitivity of the observed stress–strain behaviour to all the experimental variables except the plastic deformation amount. Craze matter structure is indeed likely to depend only on molecular characteristics of PS matrix, rubber-phase structure possibly affecting only craze number and dimensions. Moreover, a rubber-like behaviour of craze matter could be conceivable in the light of the particularly high molecular mobility existing within the fibrillar structure[8]. However, such a hypothesis would require not only an explanation for the observed discrepancy between ϕ_Y and ϕ (i.e. between craze extension ratio at Y and corresponding rubber-like matter extension ratio), but also a complete model for the deformation behaviour of craze matter structure, whose characteristics are very different from those of a crosslinked molecular network (as an example, the craze density is decreasing with increasing craze deformation).

It is, of course, possible that both rubber-phase particles and craze matter participate in the mechanical response of the yielded material, in which case an elaborate model for yielded HIPS would be necessary. In any case, a correct interpretation of the observed stress–strain behaviour should also provide an explanation for the large differences in yield stress and elongation at break resulting from the two rubber-phase structures taken into consideration (see *Figures 3* and *4*).

ACKNOWLEDGEMENTS

The authors wish to thank Ms K. Pisoni for her kind assistance in performing the experiments, and Dr G. Cigna, Dr A. G. Rossi, Dr A. Callaioli and Dr G. P. Ravanetti for helpful discussions.

REFERENCES

1 Kambour, R. P. *J. Polym. Sci. (A)* 1965, **3**, 1713
2 Kambour, R. P. *J. Polym. Sci. (A-2)* 1966, **4**, 349
3 Schirrer, R. *J. Mater. Sci.* 1987, **22**, 2289
4 Beahan, P., Thomas, A. and Bevis, M. *J. Mater. Sci.* 1976, **11**, 1207
5 Sauer, J. A. and Chen, C. C. *Adv. Polym. Sci.* 1983, **52/53**, 169
6 Bucknall, C. B. 'Toughened Plastics', Applied Science, London, 1977
7 Wool, R. P. and O'Connor, K. M. *Polym. Eng. Sci.* 1981, **21**(14), 970
8 Yang, A. C.-M. and Kramer, E. J. *J. Polym. Sci., Polym. Phys. Edn.* 1985, **23**, 1353
9 Yang, A. C.-M. and Kramer, E. J. *J. Mater. Sci.* 1986, **21**, 3601
10 Bucknall, C. B. and Stevens, W. W. *J. Mater. Sci.* 1980, **15**, 2950
11 Kambour, R. P. and Kopp, R. W. *J. Polym. Sci. (A-2)* 1969, **7**, 183
12 Kramer, E. J. *Adv. Polym. Sci.* 1983, **52/53**, 1
13 Edwards, S. F. and Vilgis, Th. *Polymer* 1986, **25**, 483
14 Bard, J. K. and Chung, C. I. 'Thermoplastic Elastomers', (Eds. N. R. Legge *et al.*), Hanser, Munich, 1987, p. 303